Tsai, M.-J., Schwartz, R. J., Tsai, S. Y., & O'Malley, B. W. (1975) *J. Biol. Chem. 250*, 5165–5174.
Tsai, M.-J., Ting, A. C., Nodstrom, J. L., Zimmer, W., & O'Malley, B. W. (1980) *Cell (Cambridge, Mass.) 22*, 219–230.
Tsai, S. Y., Roop, D. R., Tsai, M.-J., Stein, J., Means, A. R., & O'Malley, B. W. (1978) *Biochemistry 17*, 5773–5780.
Van Eekelen, C. A. G., & Van Venrooij, W. J. (1981) *J. Cell Biol. 88*, 554–563.
Van Venrooij, W. J., & Janssen, D. B. (1978) *Mol. Biol. Rep. 4*, 3–8.
Zieve, G., & Penman, S. (1976) *Cell (Cambridge, Mass.) 8*, 19–31.
Zieve, G. W. (1981) *Cell (Cambridge, Mass.) 25*, 296–297.

# Acid–Base Equilibrium of the Schiff Base in Bacteriorhodopsin†

S. Druckmann, M. Ottolenghi,* A. Pande, J. Pande, and R. H. Callender*

ABSTRACT: Aqueous suspensions of dark-adapted bacteriorhodopsin ($bR_{560}$) in the purple membrane of *Halobacterium halobium* are exposed to rapid jumps to high pH. Optical and resonance Raman measurements are carried out by using flow and stationary methods. Above pH $\simeq$11.5 $bR_{560}$ starts to be reversibly converted to a species absorbing at 460 nm ($bR_{460}$) characterized by an unprotonated Schiff base chromophore. Above pH $\simeq$13.0 bleaching takes place, first reversibly and subsequently irreversibly, to a species absorbing around 365 nm ($bR_{365}$). This process competes with the formation of $bR_{460}$. The p$K_a$ corresponding to the equilibrium

$$bR_{560} + H_2O \underset{k_a}{\overset{k_d}{\rightleftharpoons}} bR_{460} + H_3O^+$$

is determined as 13.3 ± 0.3. The value of the corresponding association rate constant determined from the reverse jumps (from pH 12.67 to pH 10 and 9.2) is $k_a = (3.5 \pm 0.5) \times 10^{11}$ $M^{-1}$ $s^{-1}$. Thus, starting with bR at pH 12.67 the reprotonation process is diffusion controlled as observed for homogeneous acid–base equilibria. The observed rate of dissociation when jumping from pH 6.5 to 12–13 is slower than that predicted by including the equilibrium

$$bR_{560} + OH^- \underset{k_a'}{\overset{k_d'}{\rightleftharpoons}} bR_{460} + H_2O$$

The results imply that the Schiff base is titratable in the dark, but its accessibility to external $OH^-$ ions is limited. The limitations in the significance of the "apparent" value of p$K_a$ = 13.3 observed for the Schiff base titration are discussed in light of possible alterations in the structure of bR resulting from the parallel titration of other protein groups. It is suggested that a light-induced p$K_a$ change of at least nine units takes place during the photocycle of light-adapted bR.

Bacteriorhodopsin (bR), the single protein in the purple membrane of *Halobacterium halobium*, functions as a light-driven proton pump leading to ATP synthesis [see Stoeckenius et al. (1979) for a comprehensive review]. The chromophore of the light-adapted form of bacteriorhodopsin absorbing at 570 nm ($bR_{570}$) is *all-trans*-retinal bound to the $\epsilon$-amino group of a lysine via a protonated Schiff base. The dark-adapted modification absorbs at 560 nm ($bR_{560}$) and contains a 1:1 ratio of 13-*cis*- and *all-trans*-retinal. It appears that the protonated polyene structure not only is responsible for the visible absorption of the pigment but also is directly involved in the proton pump mechanism [see Stoeckenius et al. (1979) and Ottolenghi (1980) for recent reviews].

Various models for proton pumping in bR have been recently discussed (Kalisky et al., 1981). The analysis led to a class of models in which pumping is exclusively based on light-induced p$K_a$ changes in the protein. A specific mechanism was suggested, based on the conclusion that during the photocycle the p$K_a$s of the Schiff base and of a neighboring tyrosine residue are both shifted (from above 12 and $\simeq$10, respectively) to <5.

The rates of deprotonation and reprotonation of the Schiff base and its p$K_a$ are also relevant to understanding the hydrogen–deuterium exchange mechanism in bR (Ehrenberg et al., 1980; Doukas et al., 1981). The problem is closely associated with the accessibility of the Schiff base to protons and to water molecules.

It is thus evident that proton-transfer phenomena directly involving the Schiff base play a primary role in the function of bacteriorhodopsin. However, the irreversible bleaching of the pigment at high pH (above $\simeq$12) has made it impossible to confirm that the Schiff base is titratable in the dark and has also prevented the determination of the p$K_a$ of the retinyl chromophore. In the present work we have carried out a series of continuous and stopped-flow experiments aiming to determine the p$K_a$ value as well as to observe the kinetics of deprotonation and reprotonation of the Schiff base.

## Experimental Procedures

All experiments were carried out with 1–10 $\mu$M suspensions of dark-adapted bacteriorhodopsin in purple membranes isolated from *Halobacterium halobium* strain M1. The preparation of purple membrane suspensions and the stopped-flow technique (using a Durrum mixing cell and a Beckman spectrometer) have been previously described (Becher & Cassim, 1975; Druckmann et al., 1979). Stopped-flow kinetic traces were obtained with a Biomation 610 transient recorder Absorption spectra were recorded on Cary 14 and Cary 219 spectrophotometers.

The low-temperature resonance Raman apparatus has been discussed elsewhere (Aton et al., 1980). Samples of dark-adapted bR were brought to a pH (or pD in the case of the

† From the Department of Physical Chemistry, The Hebrew University of Jerusalem, Jerusalem 91904, Israel (S.D. and M.O.), and the Department of Physics, City College of the City University of New York, New York, New York 10031 (A.P., J.P., and R.H.C.). *Received September 9, 1981; revised manuscript received May 11, 1982.* This work was supported in part by the U.S.–Israel Binational Science Foundation, by the Hebrew University, by grants from the National Institutes of Health (EYO 3142) and the National Science Foundation (PCM 79-02683), and by a City University PSC-BHE faculty award program to City College.

0006-2960/82/0421-4953$01.25/0 

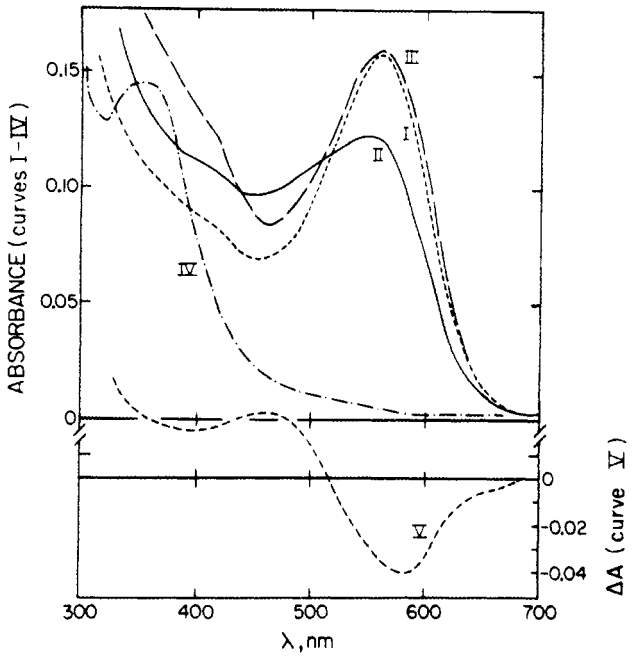


FIGURE 1: Absorbance changes induced in dark-adapted bacteriorhodopsin ($bR_{560}$) by alkalinization to pH 12.67 (10-mm cell). (Curve I) Unbuffered suspension at pH 6.5; (curve II) suspension I, 3 min after pH was raised to 12.67; (curve III) suspension II, after acidification to pH 6.2 using HCl; (curve IV) suspension II, after being allowed to stand in the dark for 15 h; (curve V) difference spectrum II − I.

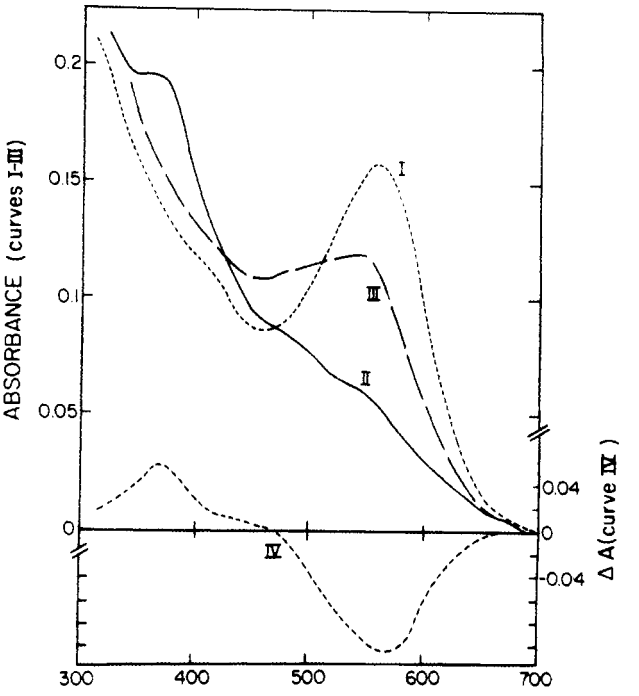


FIGURE 2: Absorbance changes induced in dark-adapted bacteriorhodopsin ($bR_{560}$) by alkalinization to pH 13.3. (Curve I) Unbuffered suspension at pH 6.5; (curve II) same suspension (I) after pH was raised to 13.3; (curve III) suspension II acidified to pH 12.6, 15 s after alkalinization; (curve IV) difference spectrum II − I.

deuterated sample) of 12.7 to produce $bR_{460}$ and subsequently cooled in the dark to 88 K in less than 7 min. Spectra, with a resolution of 9 $cm^{-1}$, were obtained by using approximately 15 mW of the 457.9-nm line of a Spectra-physics (Model 165) argon laser. The fluorescence background was subtracted as described earlier. The spectrum of $bR_{560}$ was obtained under otherwise identical conditions except that the sample was at neutral pH and the 488-nm argon laser line was used.

## Results

*General Phenomena at High pH.* Figure 1 shows the absorbance changes induced by increasing the pH of a neutral (pH ≃6.5, unbuffered) suspension of dark-adapted purple membranes (curve I). Alkalinization with NaOH to pH 12.67 (±0.03) results in a drop of the main 560-nm band with an accompanying increase in absorption below 520 nm (curve II). The corresponding difference spectrum (curve V) clearly indicates the partial conversion of $bR_{560}$ into an alkaline species characterized by an absorption maximum around 460 nm. We denote the new species as $bR_{460}$ where the subscript represents the maximum in the difference spectrum (which may slightly differ from the real absorption maximum of this species). The alkaline system corresponding to curve II is relatively unstable. After a few hours in the dark, both the 460- and (the residual) 560-nm bands are converted into a bleached suspension with maximum around 365 nm (Figure 1, curve IV). This band is assigned to a third species $bR_{365}$. The exponential kinetics associated with the generation of $bR_{365}$ ($t_{1/2}$ = 1.75 h) are shown in Figure 3V. The process is accelerated by illumination with visible light. As shown in Figure 2, alkalinization to pH values higher than ≃13 results in the immediate formation of the species absorbing around 365 nm. Under such conditions, $bR_{460}$ is barely detectable.

The process associated with the transition from $bR_{560}$ (pH ≃6.5) to $bR_{460}$ (pH 12.67 ± 0.03) was found to be reversible. Figure 1 shows that rapid acidification of the alkaline system (curve II) back to pH 6.2 essentially regenerates (curve III) the original spectrum (curve I). The discrepancy between the two curves on the high energy side is due to an increase in light scattering following both alkalinization (I → II) and acidification (II → III) steps, possibly due to changes in the ionic strength of the suspension (Reed et al., 1978). However, acidification of a suspension of $bR_{365}$ generated a few hours after alkalinization to pH 12.67 ± 0.03 did not restore the original spectrum of $bR_{560}$. Thus, under these conditions, the transition to $bR_{365}$ is irreversible, in variance with that associated with $bR_{460}$. The reversibility of the transition to $bR_{365}$ appears to depend on the time interval between alkalinization (i.e., $bR_{365}$ formation) and acidification. Thus, as shown in curve III of Figure 2, a visible absorption could be restored when a suspension of $bR_{365}$ (pH 13.3) is acidified back to pH 12.6, within 30 s after alkalinization. The effect was not observed when acidification was carried out after 5 min. Note that the spectrum of the regenerated system (Figure 2, curve III) is essentially identical with that (Figure 1, curve II) of a suspension brought to the same pH directly from pH ≃6.5. Similar to the behavior in Figure 1, further acidification of the pH 12.6 suspension restores the original absorption of $bR_{560}$. To differentiate between the two forms of $bR_{365}$, we denote by $bR_{365}^{rev}$ and $bR_{365}^{irr}$ the reversible and irreversible species, respectively.

*Kinetics of $bR_{460}$ and $bR_{365}$ Formation.* The kinetics associated with the generation of $bR_{460}$ and $bR_{365}$ were investigated by using the stopped-flow apparatus. Characteristic traces showing the generation of $bR_{460}$ are shown in Figure 3 (curves I and II). A neutral suspension of $bR_{560}$ is mixed in the stopped-flow cell with 0.1 N NaOH to yield an alkaline suspension at pH 12.67 ± 0.03. It is to this suspension that the initial base lines in Figure 3 (I and II) correspond. The introduction of a fresh mixture of $bR_{560}$ and NaOH leads to a sharp drop (absorbance increase) at 560 nm and to a sharp rise (absorbance decrease) at 460 nm. Subsequently a decay of the 560-nm band (trace growing-in) is observed, accom-

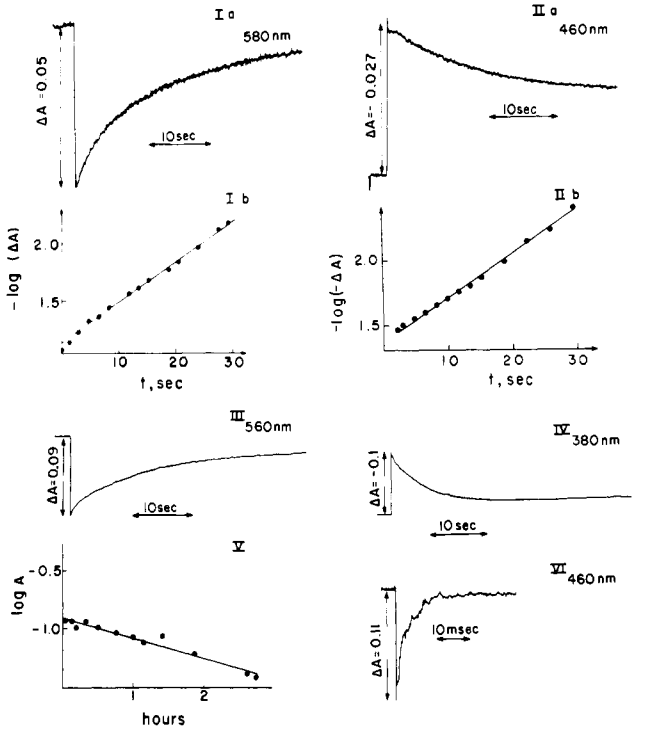


FIGURE 3: Time evolution of spectral changes induced in $bR_{560}$ by alkalinization detected in the stopped-flow apparatus. The initial segment in each trace (preceding the sharp change due to mixing) refers to the absorbance of the final alkalinization products obtained in the previous experiment. Note that the vertical scale for each trace is linear with the transmittance of the suspension. $\Delta A$'s are the calculated absorbance changes. An upward change corresponds to an increase in transmittance and to a decrease in absorbance. The pH values after a neutral bR suspension is mixed with NaOH are 12.67 (I and II) and 13.4 (III and IV). Curve Ia,b shows the transmittance change of 580 nm (a) and the corresponding kinetic plot (b) using the transmittance value after 40 s as the base line (see text). The same applies to curve IIa,b at 460 nm. (Curve V) Kinetics of the decay of the $bR_{560} \rightleftarrows bR_{460}$ equilibrium pair into $bR_{365}$ at pH 12.67 (absorbance measured on the Cary 219 spectrophotometer at 560 or 460 nm); (curve VI) the back $bR_{460} \rightarrow bR_{560}$ reaction at pH 9.2, following the acidification from pH 12.67.

panied by evolution of the absorbance around 460 nm (trace decay). However, as best seen in curve IIa of Figure 3, completion of this reaction does not regenerate the original base line. The latter is recovered only after $\simeq$3 min. This effect is mostly due to the relatively slow increase in the scattering of the suspension resulting from aggregation. This point is clearly made evident by the corresponding difference spectra shown in Figure 4. The total difference spectrum (I) corresponds to that measured on the Cary 14 spectrophotometer $\simeq$3 min after mixing (Figure 1, curve V) in the static experiments. Curve II is the net contribution of the $bR_{560} \rightarrow bR_{460}$ reaction, while curve III represents mostly the change in scattering, with some residual contribution by a slow phase of the $bR_{460}$ generation process. The kinetics of the $bR_{560} \rightarrow bR_{460}$ process as shown in Figure 3 (curves Ia and IIa) were analyzed by taking the transmittance value at the end of the fast initial decay ($\sim$40 s) as base line. First-order plots for both wavelengths are shown in Figure 3 (curves Ib and IIb). They both yield a value of $k_d(\text{obsd}) = 0.08 \pm 0.02\ s^{-1}$, in keeping with the conclusion that $bR_{560}$ decays into $bR_{460}$.

As mentioned above, $bR_{460}$ was not observed as a relatively stable alkalinization product in the stationary spectrophotometric measurements above pH $\simeq$13.2. Stopped-flow experiments indicate that, in this pH range, $bR_{460}$ is not generated, even as a transient precursor in the formation of $bR_{365}$. Figure 3 (III and IV) shows jumps to pH 13.4 monitored at

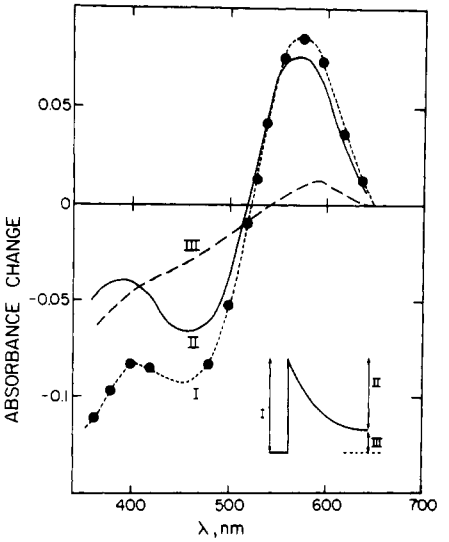


FIGURE 4: Difference spectra recorded in stopped-flow alkalinization experiments in aqueous suspensions of $bR_{560}$. The three curves correspond to the three corresponding portions of the kinetic traces (see Figure 3) as shown schematically in the insert.

560 and 380 nm. In this case alkalinization initiates a process in which $bR_{560}$ directly and quantitatively decays into $bR_{365}$. No faster stage attributable to the formation of $bR_{460}$ could be observed.

Experiments were also carried out in which alkaline suspensions at pH 12.67 were exposed to a negative pH jump so as to monitor the kinetics of the reverse $bR_{460} \rightarrow bR_{560}$ process. Jumps to pH values of 7.0, 9.2, and 10.0 resulted in first-order half-lives of <1 (below the time resolution of the stopped-flow experiments), $\simeq$3 (see Figure 3VI), and $\simeq$15 ms, respectively. The results are consistent with an observed pseudo-first-order rate constant of the form $k_a(\text{obsd}) \simeq 20 + (3.5 \times 10^{11})[H_3O^+]\ s^{-1}$; this is used in our analysis below (see Discussion).

*Reaction Scheme for the Alkalinization of Bacteriorhodopsin.* The results presented above indicate that alkalinization of $bR_{560}$ to pH values within the 11.5–13.0 range leads to the formation of the relatively stable $bR_{460}$. The reversibility of the process upon acidification and the pH dependence of the degree of conversion into $bR_{460}$ (see below) are consistent with the establishment of a pH-dependent equilibrium between $bR_{560}$ and $bR_{460}$. Both subsequently decay into $bR_{365}$. In more alkaline solutions the formation of $bR_{460}$ is inhibited by a process leading directly to $bR_{365}$. The results are consistent with Scheme I[1] in which $k_d$ (obsd) and $k_a$ (obsd) represent the corresponding (observed) forward and reverse rate constants for $bR_{460}$ formation. $bR_{560}$* represents a short-lived alkaline form of bacteriorhodopsin (so far spectroscopically indistinguishable from $bR_{560}$) that is a precursor of $bR_{365}^{rev}$ above pH $\simeq$13.0. Its presence must be invoked to account for the observation that the generation of $bR_{460}$ is inhibited above pH $\simeq$13.0 by the process forming $bR_{365}^{rev}$ which exhibits a comparable rate. (Note that $k_d$(obsd)

[1] An alternative scheme such as

$$bR_{560} \underset{k_{-1}}{\overset{k_1}{\rightleftharpoons}} bR_{460} \underset{k_{-2}}{\overset{k_2}{\rightleftharpoons}} bR_{365}^{rev} \rightarrow bR_{365}^{irr}$$

in which at pH $\simeq$13.2 $bR_{460}$ is a short-lived (unresolved) intermediate between $bR_{560}$ and $bR_{365}$, can also be suggested. We note, however, that this mechanism implies that, at this (high) pH, $k_2 \gg k_1, k_{-1}$, i.e., $k_2 \gtrsim 0.5\ s^{-1}$ as compared with $k_2 < 10^{-4}\ s^{-1}$ below pH 13 (see text). Such a drastic change in $k_2$ over a narrow pH range is unlikely, thus making the mechanism suggested in the text considerably more feasible.

Scheme I

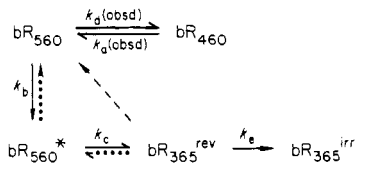


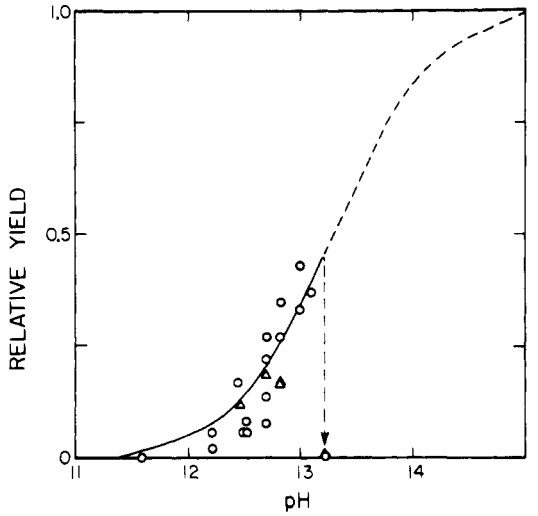


FIGURE 5: Dependence of the relative yield of $bR_{460}$, defined as $\Delta A_{460}/\Delta A_{460}^{max}$, generated by alkalinization of $bR_{560}$ on calculated pH (see text for evaluation of $\Delta A_{460}^{max}$). Experimental values determined from stopped-flow (Δ) and stationary (O) experiments, respectively. The latter involved measurements carried out within 3 min after mixing with NaOH. The S-shaped curve is the calculated titration curve for a single acid with $pK_a$ = 13.3.

$\simeq 8 \times 10^{-2}$ $s^{-1}$ while $k_c = 1.0 \times 10^{-1}$ $s^{-1}$ at pH 13.4.) In other words, it is the (unresolved) transition to $bR_{560}$* that competes with the formation of $bR_{460}$ above pH $\simeq$13.0. Since the generation rate of $bR_{460}$ is only weakly pH dependent over the 11.5 < pH < 13.0 range, the very efficient inhibition of the process above pH $\simeq$13.0 should be attributed to an extremely sharp increase in $k_b$ in this range. Thus, below pH $\simeq$13.0 $k_b < k_d$(obsd) while above pH $\simeq$13.0 $k_d$ $k_d$(obsd) $k_b$, where $k_d$(obsd) $\simeq$ 0.08 $s^{-1}$. Obviously, there is no way in which we could determine the value of $k_b$ in this critical region.

It is possible that the path via $bR_{560}$* is responsible for the slow decay of the equilibrium pair $bR_{560} \rightleftarrows bR_{460}$ into $bR_{365}$ below pH $\simeq$13 (Figure 3V). The dotted arrows in the scheme may account for the regeneration path of $bR_{560}$ from $bR_{365}^{rev}$ upon acidification. Alternatively, $bR_{365}^{rev}$ may directly convert to $bR_{560}$, circumventing $bR_{560}$* (dashed line). We finally note that no quantitative analysis of the rate of the irreversible denaturation process ($k_e$) has been carried out at the present stage of the investigation.

*pH Dependence of the $bR_{560} \rightleftarrows bR_{460}$ Equilibrium.* Experiments were carried out aiming to determine the relative amount of $bR_{460}$ within the 11.5 < pH < 13.0 range in which its equilibration with $bR_{560}$ is attainable. The results are shown in Figure 5. In choosing the relative scale in Figure 5, we assumed that completion of the evolution of $bR_{460}$ to its maximum value, $\Delta A_{460}^{max}$, is inhibited by the process leading to $bR_{560}$*. Thus, $\Delta A_{460}^{max} = \Delta A_{560}^{max}$ $(\Delta A_{460}/\Delta A_{560})$ where $\Delta A_{560}^{max}$ is the initial absorbance of $bR_{560}$ at 560 nm, prior to alkalinization. $\Delta A_{460}$ and $\Delta A_{560}$ are the absorbance changes at 460 and 560 nm, respectively, induced by alkalinization as determined in characteristic experiments (stationary, e.g., Figure 1, or stopped flow, e.g., Figure 3). Note the sharp drop in the relative yield of $bR_{460}$ around pH 13.0 in Figure 5 due to the process leading to $bR_{365}$.

*Identification of $bR_{460}$: Resonance Raman Experiments.* The reversible equilibrium between $bR_{560}$ and $bR_{460}$ at high pH (see also Discussion) strongly suggests the involvement of an acid–base reaction between two forms of bacteriorhodopsin. The question obviously arises as to the group directly involved in the titration. The well-known spectroscopic sensitivity of rhodopsins to deprotonation of the Schiff base, as well as to changes in the environment of the (protonated) retinyl moiety (Nakanishi et al., 1980), suggests that either factor might be involved. For example, in the specific case of light-adapted bacteriorhodopsin, a large blue shift, to 412 nm, is associated with the $M_{412}$ intermediate of the photocycle in which the Schiff base is unprotonated (Lewis et al., 1974; Aton et al., 1977; Braiman & Mathies, 1980). A marked red shift to 605 nm in the absorption maximum is induced by acidification of bR to pH 3 (Mowery et al., 1979), a process attributed to protonation of a negatively charged protein residue in the vicinity of the (protonated) Schiff base (Warshel & Ottolenghi, 1979; Fischer & Oesterhelt, 1980). Thus $bR_{460}$ may be identified as a protonated Schiff base with an absorption shifted by protein conformational changes induced by high pH. Alternatively, its blue-shifted absorption relative to $bR_{560}$ may

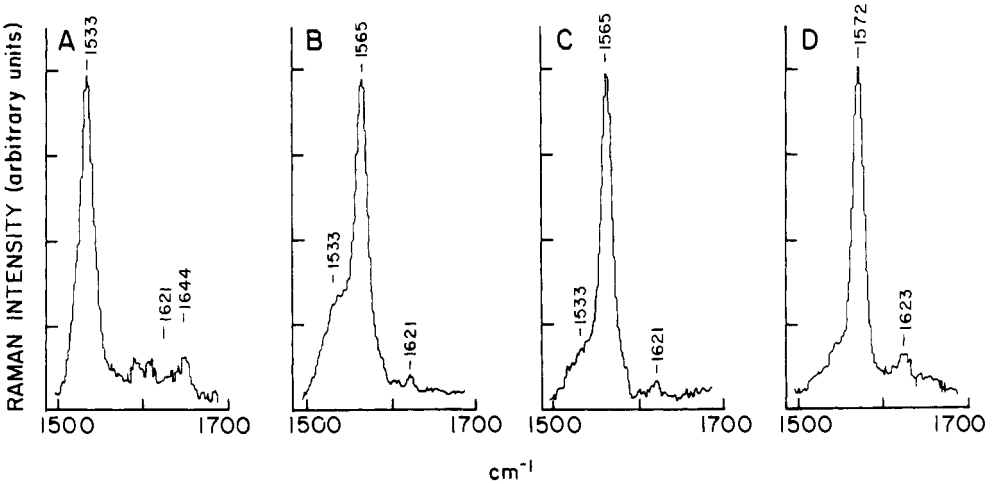


FIGURE 6: Resonance Raman spectra of bacteriorhodopsin systems. (A) $bR_{560}$; (B) $bR_{460}$; (C) deuterated $bR_{460}$; (D) $M_{412}$. Spectrum A was taken by using the 488.0-nm $Ar^+$ laser line. The 457.9-nm line was used in (B) and (C). Spectrum D is adapted from Aton et al. (1977) (see text for details).

be caused by deprotonation of the Schiff base.

For discrimination between the above possibilities, resonance Raman measurements were carried out at high pH with the purpose of obtaining the spectrum of $bR_{460}$. Figure 6 (A and B, respectively) shows the resonance Raman spectrum of $bR_{560}$ at pH 7 and that of the same suspension, mixed with NaOH to yield pH 12.65 and then rapidly cooled to 88 K. As confirmed by the insensitivity of the Raman spectra to prolonged irradiations, this method allows trapping of $bR_{460}$ as a thermally and photochemically stable species. Raman spectra were subsequently collected over a period of up to 2 h by using 457.9-nm irradiation. Figure 6C is the same as Figure 6B except that the data were collected by using a sample suspended in $D_2O$. For comparison purposes, Figure 6D shows the spectrum of $M_{412}$ (Aton et al., 1977).

The following conclusions may be derived: The characteristic 1533-$cm^{-1}$ ethylenic C=C band of $bR_{560}$ ($\lambda_{max}$ 560 nm) is replaced in $bR_{460}$ ($\lambda_{max}$ 460 nm) by one at 1565 $cm^{-1}$ and in $M_{412}$ ($\lambda_{max}$ 412 nm) by one at 1572 $cm^{-1}$. The 1565-$cm^{-1}$ value and the 460-nm maximum are in agreement with the correlation of Aton et al. (1977) between the ethylenic frequency and $\lambda_{max}$ in a variety of retinals and rhodopsins (illustrated here by the $bR_{560}$ and $M_{412}$ spectra). This confirms that spectrum 6B is mostly due to $bR_{460}$. The small contribution of $bR_{560}$ to this spectrum is attributed to the selective Raman enhancement due to the 457.9-nm line and, possibly, to favoring of the equilibrium $bR_{460}$ species at low temperatures. Examination of the high-energy range in spectrum 6B, where the C=N frequency contributes, clearly reveals a line at 1621 $cm^{-1}$ characteristic of an unprotonated Schiff base as in the case of the $M_{412}$ spectrum. The contribution of the protonated Schiff base frequency of $bR_{560}$ around 1644 $cm^{-1}$ is now absent. The assignment of the 1621-$cm^{-1}$ band of $bR_{460}$ to an unprotonated Schiff base is further strengthened by its insensitivity to sample deuteration (compare parts B and C of Figure 6).

Experiments performed at room temperature by a continuous-flow method (Doukas et al., 1981) yielded a spectrum at pH 12.65 (not shown) quite similar to the low-temperature experiments, except that a somewhat larger contribution due to $bR_{560}$ is observed. (The 1533-$cm^{-1}$ band of $bR_{560}$ and the 1566-$cm^{-1}$ band of $bR_{460}$ are of approximately equal intensity.) The low signal to noise ratio did not allow the resolution of the weak line at 1621 $cm^{-1}$. The low sensitivity in the flow experiments is due to small integration times resulting from the limited sample quantities as well as to the aggregation induced at high pH.

## Discussion

The present data indicate that at high pH, $bR_{560}$ undergoes a reversible transformation to a species, $bR_{460}$, in which the Schiff base is deprotonated. This behavior is consistent with the simple equilibrium

$$bR_{560}(\cdots C{=}N^{+}H\cdots) \rightleftarrows bR_{460}(\cdots C{=}N\cdots) + H^{+}$$

It should be noted that the 460-nm maximum is substantially red shifted relative to an unprotonated Schiff base of retinal in solution that absorbs around 380 nm [see Ottolenghi (1980) for a recent review]. It is thus evident that the interactions with the protein in the binding site markedly affect the spectrum of the unprotonated species. The effect is similar but even more pronounced than that associated with the (unprotonated) $M_{412}$ intermediate of the $bR_{570}$ photocycle, which absorbs at 412 nm.

The $bR_{460}$ generation process begins around pH 11.5 followed by a rise and then by a sharp drop around pH 13.0. Our preferred scheme accounts for such phenomena in terms of a competing process leading to $bR_{560}^{*}$ and, subsequently, via $bR_{365}^{rev}$, to the irreversible bleaching of the pigment. We assign $bR_{560}^{*}$ to an alkaline form of bacteriorhodopsin in which the path leading to $bR_{460}$ is inhibited by a considerable change in protein structure (denaturation). $bR_{365}^{rev}$ and the irreversible species $bR_{365}^{irr}$ are assigned to an unprotonated Schiff base chromophore or to a retinal resulting from hydrolysis of the C=N bond. At present, it is impossible to discriminate between the two alternatives. If the Schiff base bond in $bR_{365}$ is still intact, it is evident that the interactions which shift the spectrum of the unprotonated chomophore in $bR_{460}$ by approximately 100 nm relative to a Schiff base in solution are absent in $bR_{365}$. This indicates a substantial (though reversible) structural change of the protein in $bR_{365}^{rev}$. Larger, irreversible changes occur in the case of $bR_{365}^{irr}$.

According to the above, the experimental points representing the relative yield of $bR_{460}$ between pH 11.5 and 13.0 (Figure 5) should be regarded as the initial portion of the titration curve of the Schiff base. The experimental points coincide closely with the theoretical curve corresponding to the titration of an acid with $pK_a \simeq 13.3$. We thus conclude that the Schiff base in $bR_{560}$ is characterized by an apparent $pK_a$ of 13.3 ± 0.3. Interpretation of the actual significance of such an apparent $pK_a$ value presents two problems. First, it is in principle possible that (due to inaccessibility of the Schiff base to $H_3O^+$ and $OH^-$ ions) the curve in Figure 5 does not represent a direct titration of the Schiff base, but rather that of other groups in bR. Upon titration such groups will induce protein conformational changes which will perturb the active site, exposing the Schiff base, thus allowing its deprotonation [see Tanford (1961)]. This possibility is not favored by previous arguments (Kalisky et al., 1981), showing that the Schiff base directly participates in the proton pump mechanism and, as such, is most likely exposed to one side of the membrane. We also recall that accessibility of the retinal binding site to protons is claimed when considering the low pH form, $bR_{605}$ (Warshel & Ottolenghi, 1979; Druckmann et al., 1979).

A second problem in interpretation is that many arginines, lysines, and tyrosines are titratable at these high pH values. Such titrations may alter the Schiff base's environment, which modifies its $pK_a$. As in the case of active sites in soluble enzymes [see Ferscht (1977)], this might substantially affect the $pK_a$ value. Thus, even if the curve in Figure 5 represents a direct titration of the Schiff base, it should be considered as an "observed $pK_a$" for the condition studied. This value may be different from the actual $pK_a$ in a hypothetic titration in which only the Schiff base is deprotonated. This point should be recalled, e.g., when the light-induced $pK_a$ drop during the photocycle is considered (Kalisky et al., 1981). In any event, the "observed" shift of the $pK_a$ of the Schiff base, from solution values of ~6.5 (Favrot et al., 1978) to 13.3 in bR, is considerably larger than the shifts encountered for acidic and basic amino acids in proteins. The effect is most likely due to the stabilizing effect of a negative counterion in the vicinity of the protonated nitrogen (Honig et al., 1979). The presence of the nucleophilic group was also proposed to account for the resistance of rhodopsin Schiff bases to hydrolysis (Doukas et al., 1981).

We note that, since bR suspensions are photobleached above pH 12, no information is available concerning the degree and rates to light-to-dark adaptation in this range. Because of this, all experiments presented in the present work have been performed with the dark-adapted modification, $bR_{560}$. Preliminary experiments with purple membranes light adapted

prior to alkalinization showed a behavior qualitatively similar to the dark-adapted system, with respect to the formation of $bR_{460}$ and $bR_{365}$. More extensive work will be required when looking for differences (in $pK_a$, spectra of the corresponding $bR_{460}$ and $bR_{365}$ species, kinetic behavior, etc.) between the all-trans and 13-cis isomers of bacteriorhodopsin. It seems, however, that the general aspects of this work concerning the high pH effects, and specifically the $pK_a$ value, qualitatively apply to both isomeric chromophores.

The question arises as to the relationship between the value of the apparent $pK_a$ of the Schiff base and the corresponding protonation and deprotonation rate constants. The observed rate constants for the conversion of $bR_{560}$ into the $bR_{560} \rightleftarrows bR_{460}$ equilibrium pair [$k_d$(obsd)] and for the reverse (re-acidification) process [$k_a$(obsd)] should be considered in terms of the two equilibria:

$$HB^+ + H_2O \underset{k_a}{\overset{k_d}{\rightleftharpoons}} B + H_3O^+ \quad (1)$$

$$HB^+ + OH^- \underset{k_a'}{\overset{k_d'}{\rightleftharpoons}} B + H_2O \quad (2)$$

in which $HB^+$ represents the protonated Schiff base moiety. Because of the high pH involved in our alkalinization experiments, both reactions contribute (see below) to the dissociation process. Only the second determines the rate of the back-reaction, regenerating $bR_{560}$ from $bR_{460}$ in the reverse (acidification) pH jumps. The general expression for the rate of deprotonation, assuming that the Schiff base is as exposed to the external aqueous medium as a free acid in solution, is

$$d[B]/dt = -d[HB^+]/dt = k_d'[HB^+][OH^-] + k_d[HB^+] - k_a[B][H_3O^+] - k_a'[B]$$

leading to the expression

$$k(\text{obsd}) = k_d'[OH^-] + k_a' + k_d + k_a[H_3O^+]$$

for the rate of acid–base equilibration of the Schiff base. $k_a'$ and $k_d$ represent the pseudo-first-order rate constants involving water as an acid and as a base, respectively. Note that $k$(obsd) stands for the observed dissociation rate constant [$k_d$(obsd)] as well as for the reverse association rate constant [$k_a$(obsd)].

In terms of the corresponding equilibrium constants

$$K' = k_d'/k_a' = [B]/([HB^+][OH^-]) \quad (3)$$

$$K = k_d/k_a = [B][H_3O^+]/[HB^+] \quad (4)$$

the observed equilibration rate assumes the form

$$k(\text{obsd}) = (k_d'[OH^-] + k_d)[1 + K_w/(K[OH^-])] \quad (5)$$

where

$$K' = K/([H_3O^+][OH^-]) = K/K_w \quad (6)$$

Our observed values are $k_d$(obsd) $\simeq 0.08\ s^{-1}$ (at pH 12.67) for the dissociation reaction and $k_a$(obsd) $\simeq (20 \pm 5) + [(3.5 \pm 0.5) \times 10^{11}][H_3O^+]\ s^{-1}$ for the association process at pH 9.2 and 10. From eq 3–6, using the value of $pK_a = 13.3$ as determined from Figure 5 (i.e., $K = 10^{0.7}$), we obtain from the back jump (from pH 12.67 to pH 9.2 and 10.0) $k_a = 3.5 \times 10^{11}\ M^{-1}\ s^{-1}$, $k_a' = 20\ s^{-1}$, $k_d = 0.015\ s^{-1}$, and $k_d' = 100\ M^{-1}\ s^{-1}$. Note that in back jumps to pH $\lesssim$7, the contribution of equilibrium 2 becomes negligible. However, experiments in this time range involve $k_a$(obsd) values which are beyond the resolution (mixing time) of the stopped-flow apparatus.

In homogeneous aqueous solutions the simple relation $k_d = 10^{-pK_a} k_a$ applies. As reviewed by Eigen (1964), $k_a$ is always close to the diffusion-controlled rate constant for the recombination of protons, in the range $10^{10}\ M^{-1}\ s^{-1} < k_a < 10^{11}\ M^{-1}\ s^{-1}$. In spite of the inherent inaccuracy in the value of $k_a$, it is evident that the reprotonation process, when jumping from pH 12.67 to pH 10 or 9.2, is essentially diffusion controlled. In principle, this cannot be assumed to apply trivially to any titratable residue in proteins. Acid groups located in pockets that are only slowly equilibrated with the outside proton concentration will obviously exhibit deviations from the above expression. Our data show that the Schiff base is titratable and that at pH 12.67 it is readily accessible to outside protons. The latter conclusion follows from the value of $k_a$ that is of the order of the diffusion-controlled rate constant for a proton recombination process. We note, however, that $k_a$ is somewhat larger than the recombination rate constant corresponding to, e.g., acetic acid in water (Grunwald & Eustace, 1975). This may imply special proton funneling effects of the purple membrane (or of the bacteriorhodopsin molecule), leading to a larger apparent cross section for the diffusion-controlled reaction between protons and the Schiff base.

An inconsistency with a simple behavior of the Schiff base as a free acid in solution is encountered when the forward alkalinization process is analyzed from pH 6.5 to 12–13. When the above values of $k_d$ and $k_a$ obtained from the back pH jumps are used, the above expressions predict $k_d$(obsd) $\simeq 25\ s^{-1}$ at pH 12.67. This value is substantially higher than the measured value $k$(obsd) = $0.08\ s^{-1}$. Namely, this measured value is higher than that of the dissociation via equilibrium 1 ($k_d = 0.015\ s^{-1}$), but slower than that predicted ($25\ s^{-1}$) using both equilibria 1 and 2. This implies that the rate of reaction of the Schiff base with $OH^-$ ions upon alkalinization of a neutral suspension is much slower than that of the free acid in solution. In conclusion, it appears that the accessibility of the Schiff base to hydroxyl ions is limited by the specific protein structure.

The results presented above bear on the mechanism of hydrogen–deuterium exchange of the bacteriorhodopsin Schiff base. The value of $k_d$(obsd) is too small to account for the submillisecond exchange (Doukas et al., 1981) on the basis of a deprotonation–reprotonation mechanism. This strongly supports the process previously proposed by us in which exchange occurs by a concerted hydrogen–deuterium exchange involving a water molecule interacting directly with the Schiff base.

The most important implications of the present work are those related to the titrability of the Schiff base and to the determination of its $pK_a$. Both observations bear directly on the mechanism of proton pumping, especially on the role played in it by the Schiff base. Several observations have strongly suggested that the Schiff base moiety is not only responsible for light absorption and for energy storage (Honig et al., 1979) but also directly involved in the proton translocation process. First, the ejection of protons to the outside of the membrane occurs on a time scale comparable to the rate of $M_{412}$ formation (Lozier et al., 1976; Ort & Parson, 1978). Second, the Schiff base loses its proton during the $M_{412}$ generation process (Lewis et al., 1974; Aton et al., 1977; Braiman & Mathies, 1980). Finally, a relationship between $M_{412}$ formation and proton pumping is suggested by the observation (Lozier et al., 1978) that the 13-cis chromophore which has no blue-shifted intermediate in its photocycle (Kalisky et al., 1977) does not initiate proton pumping.

As extensively discussed by Kalisky et al. (1981), the vectorial transport of protons in the pump implies the existence of at least two states of bacteriorhodopsin, $E_i \rightleftarrows E_iH^+$ and $E_o \rightleftarrows E_oH^+$, accessible to protons from the inside and the outside of the cell, respectively. In the direct participation of the Schiff base in the vectorial transport, it is implied that the forms E

and $EH^+$ represent the unprotonated and protonated forms of the Schiff base (···=N—··· and ···=$N^+$H—···), respectively. It is thus evident that the exposure of the Schiff base to external protons, i.e., its titrability, constitutes a prerequisite for its direct participation in the proton pump. The present data are in keeping with these requirements.

The second point concerns the $pK_a$ value. Two classes of pumping mechanisms in bR have been discussed recently (Kalisky et al., 1981). The first is initiated by a light-induced change in the protein's exposure to protons, e.g.

$$E_iH^+ \xrightarrow{h\nu} E_oH^+$$

possibly because isomerizing the retinyl moiety changes the exposure of the Schiff base to protons, from the inside to the outside of the cell. Mechanisms of the second class are based on the occurrence of a light-induced change in the $pK_a$ of $E_oH^+$ (i.e., of the Schiff base), without requiring an exposure change prior to its deprotonation. The presently suggested value of $\sim$13 for the $pK_a$ in the dark, as compared with <5 during the $M_{412}$ phase of the photocycle (Kalisky et al., 1981), confirms the feasibility of a pump mechanism based exclusively on a light-induced $pK_a$ change.

We finally note that the effects observed in this work bear on the more general problem of acid–base titrations in proteins. They call for a systematic study of the correlation between the observed $pK_a$ values of protein residues and the corresponding rate parameters $k_d$(obsd) and $k_a$(obsd). Such studies may provide valuable information relative to the exposure, and thus the environment, of such residues.

Acknowledgments

We are indebted to Dr. A. Samuni for his help in the stopped-flow experiments and to Professor Perlmutter-Hayman for valuable discussions.

References

Aton, B., Doukas, A. G., Callender, R. H., Becher, B., & Ebrey, T. G. (1977) *Biochemistry 16*, 2995.

Aton, B., Doukas, A. G., Narva, D., Callender, R. H., Dinur, U., & Honig, B. (1980) *Biophys. J. 29*, 79.

Becher, B., & Cassim, J. (1975) *Prep. Biochem. 5*, 161.

Braiman, M., & Mathies, R. (1980) *Biochemistry 19*, 5421.

Doukas, A. G., Pande, A., Suzuki, T., Callender, R. H., Honig, B., & Ottolenghi, M. (1981) *Biophys. J. 33*, 275.

Druckmann, S., Samuni, A., & Ottolenghi, M. (1979) *Biophys. J. 26*, 143.

Ehrenberg, B., Lewis, A., Porta, J. F., Nagle, J. F., & Stoekenius, W. (1980) *Proc. Natl. Acad. Sci. U.S.A. 77*, 6571.

Eigen, M. (1964) *Angew. Chem., Int. Ed. Engl. 3*, 1.

Favrot, J., Sandorfy, C., & Vocelle, D. (1978) *Photochem. Photobiol. 28*, 271.

Ferscht, F. (1977) *Enzyme Structure and Mechanism*, p 143, W. H. Freeman, San Francisco, CA.

Fischer, U. Ch., & Oesterhelt, D. (1980) *Biophys. J. 31*, 139.

Grunwald, E., & Eustace, D. (1975) *Proton Transfer Reactions* (Gold, V., & Caldin, E., Eds.) pp 103–120, Chapman and Hall, London, and Wiley, New York.

Honig, B., Ebrey, T. G., Callender, R. H., Dinur, U., & Ottolenghi, M. (1979) *Proc. Natl. Acad. Sci. U.S.A. 76*, 2503.

Kalisky, O., Goldschmidt, C. R., & Ottolenghi, M. (1977) *Biophys. J. 19*, 185.

Kalisky, O., Ottolenghi, M., Honig, B., & Korenstein, R. (1981) *Biochemistry 20*, 649.

Lewis, A., Spoonhower, J., Bogomolni, R., Lozier, R., & Stoeckenius, W. (1974) *Proc. Natl. Acad. Sci. U.S.A. 71*, 4462.

Lozier, R. H., Niederberg, W., Bogomolni, R. A., Hwang, S.-B., & Stoeckenius, W. (1976) *Biochim. Biophys. Acta 440*, 545.

Lozier, R. H., Niederberger, W., Ottolenghi, M., Sivorinovsky, G., & Stoeckenius, W. (1978) *Dev. Halophilic Microorg. 1*, 103.

Mowery, P. C., Lozier, R. H., Chae, Q., Tseng, Y.-W., Taylor, M., & Stoeckenius, W. (1979) *Biochemistry 18*, 4100.

Nakanishi, K., Balogh-Nair, V., Arnobaldi, M., Tsujimoto, K., & Honig, B. (1980) *J. Am. Chem. Soc. 102*, 7945.

Ort, D. R., & Parson, W. W. (1978) *J. Biol. Chem. 253*, 6158.

Ottolenghi, M. (1980) *Adv. Photochem. 12*, 97.

Reed, T., Hess, B., & Dostor, W. (1978) *Biochim. Biophys. Acta 502*, 188.

Stoeckenius, W., Lozier, R. H., & Bogomolni, R. A. (1979) *Biochim. Biophys. Acta 505*, 215.

Tanford, C. (1961) in *Physical Chemistry of Macromolecules*, p 555, Wiley, New York.

Warshel, A., & Ottolenghi, M. (1979) *Photochem. Photobiol. 30*, 291.